Waveguide Magnetic Resonance Elastography in a Pressure-Varying Porcine Model

Ria Mazumder[1,2]

[1]Department of Electrical and Computer Engineering

[2]Department of Radiology

The Ohio State University

Abstract

Purpose:

To determine anisotropic myocardial stiffness using waveguide cardiac magnetic resonance elastography (CMRE) in an *ex-vivo* porcine model with varying left ventricular pressure simulating heart failure with preserved ejection fraction and compare the results against isotropic myocardial stiffness.

Methods

Diffusion tensor imaging (DTI) and CMRE was implemented on three *ex-vivo* porcine hearts inflated with two different pressure values on a 3T MRI scanner to obtain fiber orientation and displacement information respectively. An orthotropic inversion was performed on the displacement data to estimate the anisotropic stiffness coefficients (compressional and shear) in the heart for both the inflation pressures and the results were compared against isotropic stiffness estimates. Paired student's t-test was performed to determine the significant difference in stiffness values between the two inflation pressures with the two different inversion techniques.

Results

Our results show that anisotropic stiffness estimates demonstrated a significant difference between the two inflation pressures both in the compressional (P-Value=0.0053) and shear (P-Value=0.0015) measurements. On the other hand, the isotopic stiffness measurements showed a minute slight increase in stiffness as a function of pressure with no significant difference (P-value=0.75).

Conclusion

From the results we can conclude that it is feasible to estimate anisotropic stiffness in the myocardium and anisotropic myocardial stiffness provides superior information as compared to isotropic myocardial stiffness.

Keywords

Anisotropic myocardial stiffness (AMS), Isotropic myocardial stiffness (IMS), waveguide cardiac magnetic resonance elastography (CMRE), diffusion tensor imaging (DTI).

INTRODUCTION

Myocardial stiffness (MS) [1-4] is an important parameter in determining cardiac function. Stiffness is elevated in cardiovascular diseases such as ischemia [5], myocardial infarction (MI) [6], hypertension [7], diastolic dysfunction [8] and hypertrophic cardiomyopathy (HCM) [9]. These diseases trigger heart failure (HF) either with reduced or with preserved ejection fraction (HFPEF) [10]. Among 5.1 million [11] Americans with HF, 50% [12, 13] suffer from HFPEF. Although, epidemiological studies have confirmed equal prevalence of both kinds of HF [14], clinical therapies for HFPEF have not been established yet [15], precisely because there remains controversy about the diagnostic criteria for HFPEF [4, 14, 16-20], and to date no placebo-controlled trial has convincingly demonstrated morbidity or mortality reduction in HFPEF [21]. However, it is well known that HFPEF is associated with impaired left ventricular (LV) relaxation due to increased passive MS [22-25]. The current gold standard for assessing MS [1, 26-28] is pressure-volume (P-V) analysis which is invasive in nature, requires technical precision and measures LV chamber stiffness which does not indicate the true intrinsic property of the myocardium. The other commonly used technique to estimate MS known as mechanical testing requires ex-vivo strips and cannot provide information of MS during heart cycle [29-32].

With the advent of medical imaging non-invasive surrogates such as Doppler-echocardiography (DE), ultrasound elastography (UE) [33, 34] and MRI based techniques like spatial modulation of magnetization tagging [35, 36], strain encoding [37] and displacement encoding with stimulated echo [38] became popular. While the predictive accuracy of DE is suboptimal [23, 39], UE has not been applied to estimate MS and the MRI based techniques only measures cardiac deformity (strain) and does not consider loading conditions (stress) and hence does not provide a true estimate of MS.

Therefore, there is a need to non-invasively quantify MS to understand the pathophysiology of HFPEF. Furthermore, investigating anisotropic myocardial stiffness (AMS) will additionally enhance diagnosis and prognosis of HFPEF primarily due to 2 reasons. First, disease progression in HFPEF is associated to increase in AMS. This is because factors triggering HFPEF like aging [40] and diabetes [41] related to increase in MS are caused by increase in cross-linking (C-L) of extra cellular matrix (ECM) fibrillar collagen [42]. This deposition of C-L of ECM causes an increase in MS and occurs with pronounced preference in the direction transverse to the myocardial fibers [43]. Second, any insight about the anisotropic pathway of disease progression in HFPEF will assist in development of therapy specific to HFPEF. This is because, there is evidence that some myocardial therapeutic agents provide anisotropic therapeutic effect [44, 45]. Moreover other agents have been known for breaking down the C-L of ECM leading to decreased MS that prevented myocardial complications associated with aging, hypertension and diabetes. Combination of these properties of drugs can be exploited to treat affected anisotropic pathways in HFPEF.

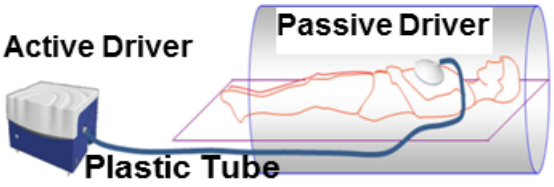

Figure 1: Schematic of a CMRE set-up. An active acoustic driver is placed outside the scan room. A passive driver is placed on the chest wall. Acoustic waves are transmitted from the active driver to the passive driver via a tube and finally induced into the myocardium.

Cardiac magnetic resonance elastography (CMRE), pioneered in our lab is the first non-invasive technique to quantify MS [46-55]. CMRE involves a

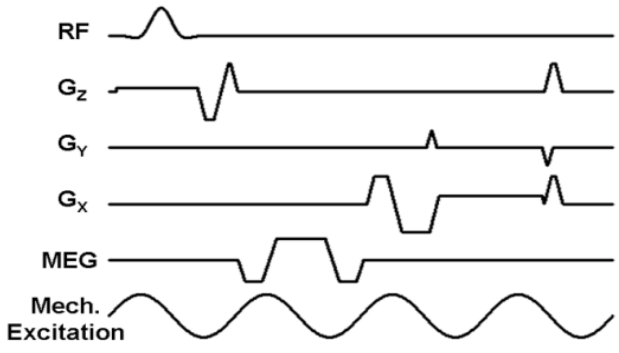

Figure 2. A GRE based CMRE sequence showing that the motion encoding gradients (MEG) are synchronized with the external excitation. The MEG can be applied along any axis.

3 stage process. First, acoustic waves are introduced through the chest wall into the myocardium (Fig. 1). Next, a phase-contrast MRI sequence (Fig. 2) is synchronized with the externally-applied waves to encode the wave displacements. Finally, the displacements are converted to stiffness maps through a mathematical process called inversion. Existing CMRE inversion algorithms [56] assume that the induced acoustic waves are propagating in a uniform, infinite, homogenous, isotropic medium. Therefore, current inversions provide only a coarse estimate of isotropic myocardial stiffness (IMS). Further advancement in CMRE is feasible by incorporating myocardial anisotropy into the inversion algorithm.

Recently, with the development of waveguide CMRE a novel inversion algorithm to explore AMS has been defined [57]. Waveguide CMRE explores the inherent property of tissues to support anisotropic wave propagation in order to estimate AMS. This concept was first introduced by Romano et al. in 2005 [58] using a stalk of celery. It was later implemented on a human volunteer to estimate anisotropic stiffness in calf muscles [59]. In 2012, the technique was applied to measure in-vivo anisotropic stiffness of brain white matter tracts [60] and then later applied on amyotrophic lateral sclerosis patients [61]. In this study, we implement waveguide CMRE to determine AMS and IMS in an ex-vivo porcine model with varying left ventricular pressure simulating a heart failure model with preserved ejection fraction and show that AMS provides superior information compared to IMS.

METHODS

Waveguide CMRE

Waveguide CMRE is based on the inherent anisotropic property of biological tissues to support anisotropic wave propagation which is exploited to estimate AMS. The *inversion* algorithm requires a prior knowledge of the fiber pathways along which acoustic waves travel

within the myocardium, in a particular volume surrounding these pathways. The orientation of the pathways is identified using diffusion tensor imaging (DTI) and the dynamic displacements are provided by the CMRE acquisition. Provided with the knowledge of the position vectors of the pathways a spatial-spectral filter is applied to the first harmonic displacement data in order to isolate waves traveling in specific directions parallel and orthogonal to the myocardial fibers. Simultaneously, Helmholtz decomposition will be implemented to separate the total field into its longitudinal and transverse components. By filtering the displacements along the six specific directions within the local reference frame (Fig. 3) of the fibers, the equations of motion decouple allowing each of the nine elastic coefficients to be solved independently of one another. Finally, an orthotropic inversion is implemented on the filtered longitudinal and transverse displacements to evaluate the stiffness coefficients along the diagonals of the orthotropic tensor. The compressional (C_{11}, C_{22}, C_{33}) and shear (C_{44}, C_{55}, C_{66}) complex stiffness values along the diagonals are computed using the following equations.

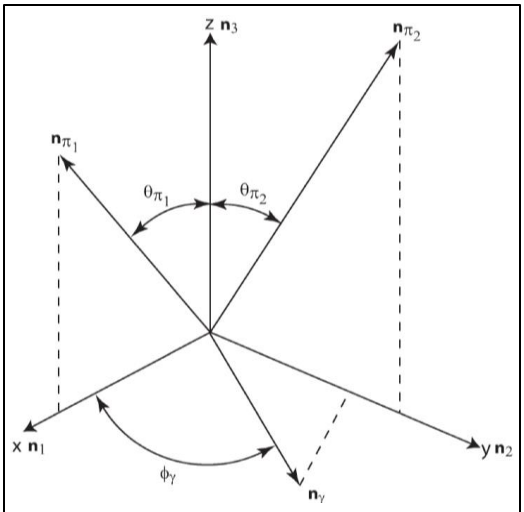

Figure 3: Local reference frame of the fiber tracts constructed from the principal eigenvector.

Along the n_1 direction of the local reference frame the compressional and shear components are given by:

$$C_{11}\,\frac{\partial^2 u_1^L(n_1)}{\partial x_1^2} = -\rho\omega^2 u_1^L(n_1) \tag{1a}$$

$$C_{66}\,\frac{\partial^2 u_2^T(n_1)}{\partial x_1^2} = -\rho\omega^2 u_2^T(n_1) \tag{1b}$$

$$C_{55}\,\frac{\partial^2 u_3^T(n_1)}{\partial x_1^2} = -\rho\omega^2 u_3^T(n_1) \tag{1c}$$

Along the n_2 direction of the local reference frame the compressional and shear components are given by:

$$C_{66}\ \frac{\partial^2 u_1^T(n_2)}{\partial x_2^2} = -\rho\omega^2 u_1^T(n_2) \tag{2a}$$

$$C_{22}\ \frac{\partial^2 u_2^L(n_2)}{\partial x_2^2} = -\rho\omega^2 u_2^L(n_2) \tag{2b}$$

$$C_{44}\ \frac{\partial^2 u_3^T(n_2)}{\partial x_2^2} = -\rho\omega^2 u_3^T(n_2) \tag{2c}$$

Along the n_3 direction of the local reference frame the compressional and shear components are given by:

$$C_{66}\ \frac{\partial^2 u_1^T(n_2)}{\partial x_2^2} = -\rho\omega^2 u_1^T(n_2) \tag{3a}$$

$$C_{22}\ \frac{\partial^2 u_2^L(n_2)}{\partial x_2^2} = -\rho\omega^2 u_2^L(n_2) \tag{3b}$$

$$C_{44}\ \frac{\partial^2 u_3^T(n_2)}{\partial x_2^2} = -\rho\omega^2 u_3^T(n_2) \tag{3c}$$

Where $u_1(n_1)$, $u_2(n_2)$ and $u_3(n_3)$ represent the directionally filtered displacements provided by the spatial-spectral filter; x_1, x_2, x_3 are the differential parameters along the rotated axes, and the superscripts L and T correspond to the longitudinal and transverse components provided by the Helmholtz decomposition.

Experimental Set-up

Three juvenile Yorkshire (~80 lbs) pigs were used for this study. After the animals were euthanized, their hearts were extracted, flushed and stored in

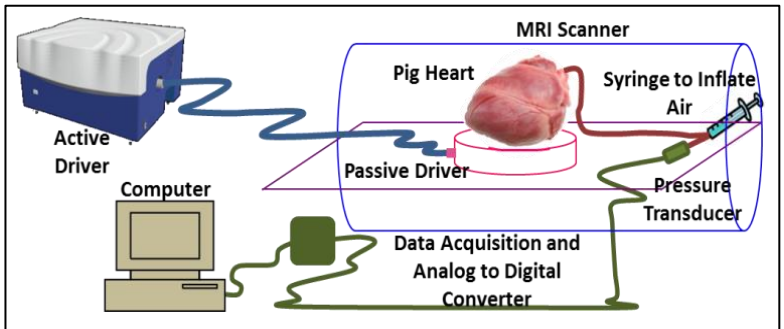

Figure 4. Experimental set-up.

Ringer's solution at 4°C till the scanner was available (i.e. ~5 hrs). A balloon was inserted through the aortic opening into the LV chamber via a plastic tube (Fig. 4). The other end of the plastic tube was connected to a T-connector. A syringe was attached to one end of the T-connection to inflate the balloon with air at two different inflation pressures as shown in Fig. 5. Pressure ranges varied from 50 to 70mm of Hg for the lower inflation and 80 and 110mm of Hg for the higher inflation. The other end of the T-connection was connected to a pressure transducer (PX26-005GV, Omega Engineering, Stamford, CT) to measure the real-time pressure in the heart using a computer at a sampling rate of 1kHz.

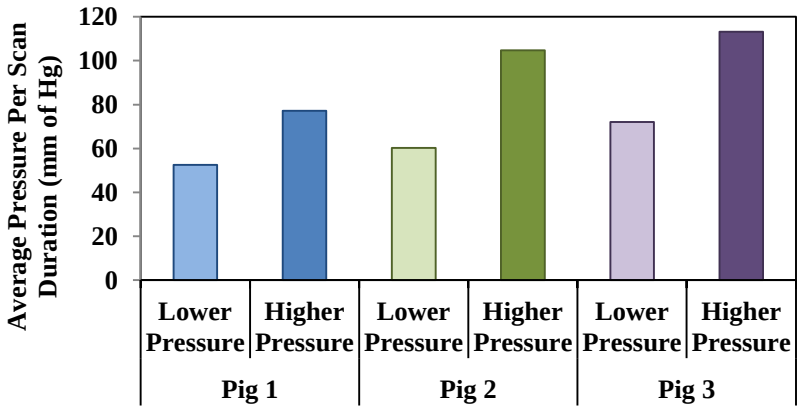

Figure 5: Chart showing inflation pressures

Acquisition

DTI and CMRE were performed on 3 *ex-vivo* pig hearts on a 3T MRI scanner (Tim Trio, Siemens Healthcare, Erlangen, Germany). Short axis views covering the entire myocardium were imaged at an isotropic resolution of 2x2x2mm (imaging matrix: 128x128 mm^2; FOV: 256x256mm^2). ***DTI:*** Imaging parameters included: 30 diffusion encoding directions; 4 averages; TE/TR=90/5000ms; b-values=0,1000s/mm^2; ***MRE:*** Imaging parameters included: TE/TR=23.3ms/33.33ms; $\alpha=22^o$; mechanical vibration frequency=60Hz; 4 MRE time offsets; and motion encoding gradients (MEG) of 16.67ms duration (60Hz) was applied in all the three directions (x, y, z) to encode the in-plane and through plane motion. Positive and negative MEG

amplitudes were used on alternate views and a phase contrast reconstruction was performed to obtain images of tissue displacement.

Analysis

The acquired MRE and DTI images were masked to segment the LV. Custom-built software written in Matlab (Mathworks, Natick, MA) was used to obtain the principal eigenvectors. A spatial-spectral filter and the Helmholtz decomposition were applied to the displacements over a volume of 8 X 8 X 8 pixels (x,y,z) about the fiber to provide the filtered displacements at each data point using a Cooley-Tukey wavenumber filter with $\Delta k=1$. The necessary spatial derivatives were subsequently performed in k-space, and inversions of the previous equations were performed in real space yielding the complex elastic coefficients for AMS. Additionally, isotropic stiffness was measured using MRE Lab (Mayo Clinic, Rochester, MN). A 3D local frequency estimation (LFE) inversion [56] was performed by applying a directional filter in 8 directions (to remove the reflected waves) and a band-pass filter (to remove the longitudinal motion). The mean AMS and IMS values and their standard deviation (SD) from all the slices were reported. Paired student's t-test was performed to determine the significant difference in stiffness values between the two inflation pressures with the two different inversion techniques.

RESULTS AND DISCUSSION

Figure 6 shows the wave image and the corresponding stiffness maps (anisotropic and isotropic) for Pig 1 at two different inflation pressures. From the stiffness maps we observe that results corresponding to higher inflation pressure have higher stiffness estimates as compared to lower inflation pressure. A quantitative analysis of all the pigs is shown in a bar graph in Fig. 7. The mean stiffness values and their standard deviations for both the anisotropic (C11-C66) and

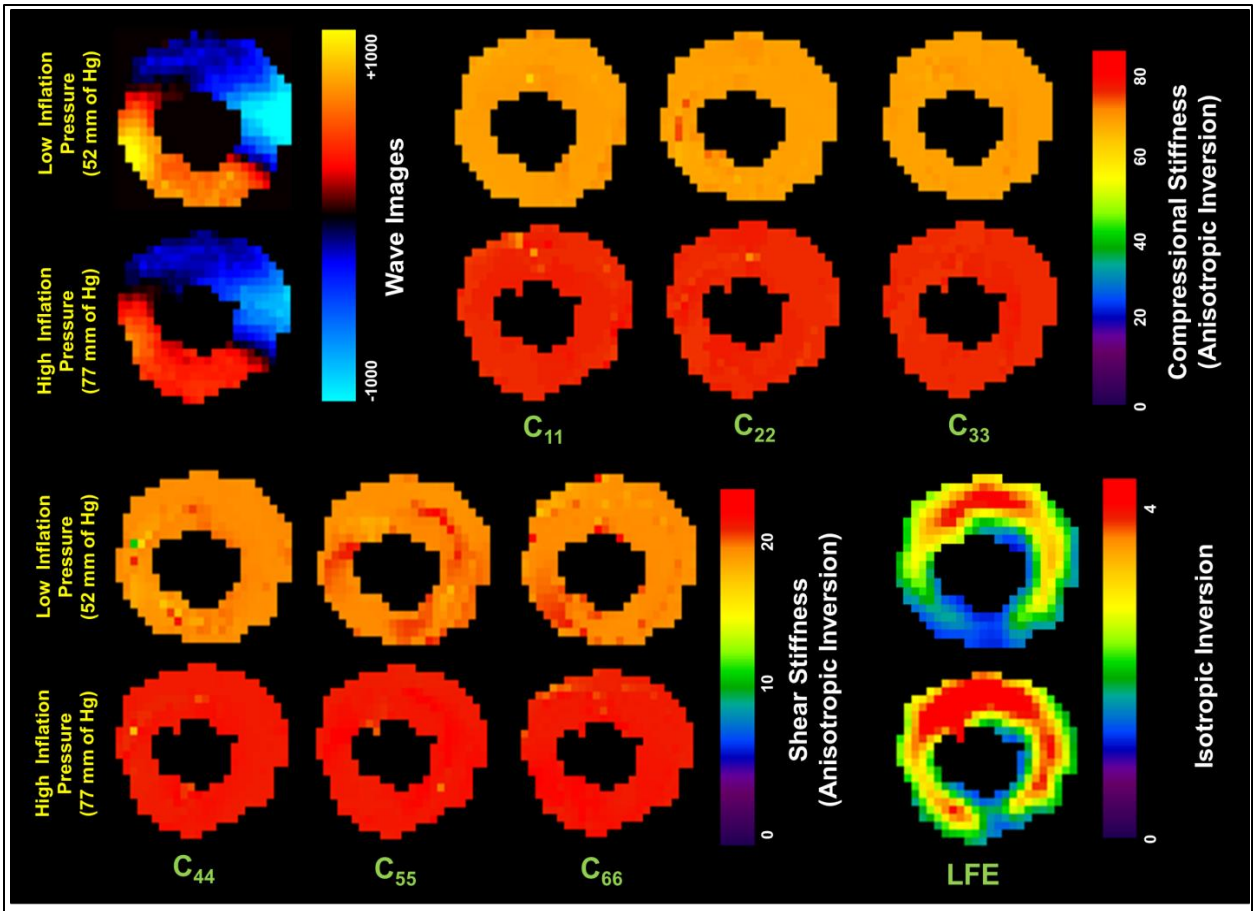

Figure 6. Wave images, anisotropic stiffness maps and isotropic stiffness maps from Pig 1 for both the lower and higher inflation pressures. The wave image shows wave propagation in X-direction.

isotropic inversion (LFE) algorithms in all the porcine hearts have been reported in the graph. In all the cases our results demonstrate that in general, compressional stiffness coefficients (C_{11}, C_{22}, and C33) are higher than the shear stiffness coefficients (C_{44}, C_{55}, C_{66}) which are higher than the isotropic stiffness measurements. Furthermore, we observed that there was a significant difference between the stiffness measurements of the lower inflation pressure and the higher inflation pressure for the anisotropic inversion model. The P-value for the compressional coefficients was 0.0053 and the P-value for the shear coefficients was 0.0015. However, the isotopic stiffness coefficients indicated a minute increase in stiffness as a function of pressure with no significant difference (P-value=0.75).

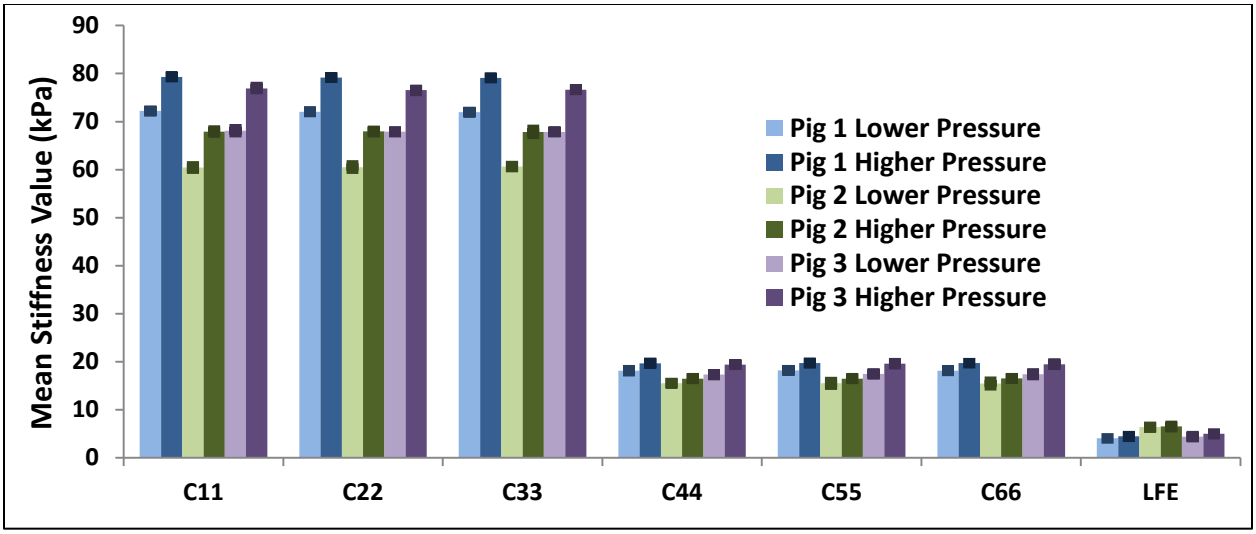

Figure 6. Columns 1-3: Mean and SD for compressional stiffness coefficients (C_{11}- C_{33}). Columns 4-6: Mean and SD for shear stiffness coefficients (C_{44}- C_{66}). Column 7: Mean and SD for isotropic shear stiffness measured using local frequency estimation. Colors blue green and purple corresponds to Pig 1, Pig 2 and Pig 3 respectively. The lighter shades represent stiffness measurements from lower pressure values and the darker shades represent stiffness measurements from higher pressure values.

CONCLUSION

In this study we have demonstrated the feasibility of determining non-invasive anisotropic stiffness along individual myocardial fibers using waveguide CMRE. We have proved that anisotropic assumptions for *inversion* model provide superior information compared to isotropic assumptions. More studies involving multiple inflation pressures are warranted to determine the reliability of this technique and its applications for the diagnosis and prognosis of different cardiac diseases especially HFPEF.

REFERENCES

[1] I. Mirsky and J. S. Rankin, "The effects of geometry, elasticity, and external pressures on the diastolic pressure-volume and stiffness-stress relations. How important is the pericardium?," *Circulation research,* vol. 44, pp. 601-11, May 1979.

[2] C. Pislaru, C. J. Bruce, P. C. Anagnostopoulos, J. L. Allen, J. B. Seward, P. A. Pellikka, E. L. Ritman, and J. F. Greenleaf, "Ultrasound strain imaging of altered myocardial stiffness: stunned versus infarcted reperfused myocardium," *Circulation,* vol. 109, pp. 2905-10, Jun 15 2004.

[3] S. Watanabe, J. Shite, H. Takaoka, T. Shinke, Y. Imuro, T. Ozawa, H. Otake, D. Matsumoto, D. Ogasawara, O. L. Paredes, and M. Yokoyama, "Myocardial stiffness is an important determinant of the plasma brain natriuretic peptide concentration in patients with both diastolic and systolic heart failure," *European heart journal,* vol. 27, pp. 832-8, Apr 2006.

[4] M. R. Zile, C. F. Baicu, and W. H. Gaasch, "Diastolic heart failure--abnormalities in active relaxation and passive stiffness of the left ventricle," *The New England journal of medicine,* vol. 350, pp. 1953-9, May 6 2004.

[5] G. M. Rosano, M. Fini, G. Caminiti, and G. Barbaro, "Cardiac metabolism in myocardial ischemia," *Current pharmaceutical design,* vol. 14, pp. 2551-62, 2008.

[6] M. G. Sutton and N. Sharpe, "Left ventricular remodeling after myocardial infarction: pathophysiology and therapy," *Circulation,* vol. 101, pp. 2981-8, Jun 27 2000.

[7] C. H. Conrad, W. W. Brooks, J. A. Hayes, S. Sen, K. G. Robinson, and O. H. Bing, "Myocardial fibrosis and stiffness with hypertrophy and heart failure in the spontaneously hypertensive rat," *Circulation,* vol. 91, pp. 161-70, Jan 1 1995.

[8] N. Hamdani and W. J. Paulus, "Myocardial titin and collagen in cardiac diastolic dysfunction: partners in crime," *Circulation,* vol. 128, pp. 5-8, Jul 2 2013.

[9] S. A. Chang, S. C. Lee, Y. H. Choe, H. J. Hahn, S. Y. Jang, S. J. Park, J. O. Choi, S. W. Park, and J. K. Oh, "Effects of hypertrophy and fibrosis on regional and global functional heterogeneity in hypertrophic cardiomyopathy," *Int J Cardiovasc Imaging,* Oct 25 2012.

[10] D. Westermann, M. Kasner, P. Steendijk, F. Spillmann, A. Riad, K. Weitmann, W. Hoffmann, W. Poller, M. Pauschinger, H. P. Schultheiss, and C. Tschope, "Role of left ventricular stiffness in heart failure with normal ejection fraction," *Circulation,* vol. 117, pp. 2051-60, Apr 22 2008.

[11] A. S. Go, D. Mozaffarian, V. L. Roger, E. J. Benjamin, J. D. Berry, M. J. Blaha, S. Dai, E. S. Ford, C. S. Fox, S. Franco, H. J. Fullerton, C. Gillespie, S. M. Hailpern, J. A. Heit, V. J. Howard, M. D. Huffman, S. E. Judd, B. M. Kissela, S. J. Kittner, D. T. Lackland, J. H. Lichtman, L. D. Lisabeth, R. H. Mackey, D. J. Magid, G. M. Marcus, A. Marelli, D. B. Matchar, D. K. McGuire, E. R. Mohler, 3rd, C. S. Moy, M. E. Mussolino, R. W. Neumar, G. Nichol, D. K. Pandey, N. P. Paynter, M. J. Reeves, P. D. Sorlie, J. Stein, A. Towfighi, T. N. Turan, S. S. Virani, N. D. Wong, D. Woo, and M. B. Turner, "Heart Disease and Stroke Statistics--2014 Update: A Report From the American Heart Association," *Circulation,* Dec 18 2013.

[12] G. C. Fonarow, W. G. Stough, W. T. Abraham, N. M. Albert, M. Gheorghiade, B. H. Greenberg, C. M. O'Connor, J. L. Sun, C. W. Yancy, and J. B. Young, "Characteristics, treatments, and outcomes of patients with preserved systolic function hospitalized for heart failure: a report from the OPTIMIZE-HF Registry," *Journal of the American College of Cardiology,* vol. 50, pp. 768-77, Aug 21 2007.

[13] C. W. Yancy, M. Lopatin, L. W. Stevenson, T. De Marco, and G. C. Fonarow, "Clinical presentation, management, and in-hospital outcomes of patients admitted with acute decompensated heart failure with preserved systolic function: a report from the Acute

Decompensated Heart Failure National Registry (ADHERE) Database," *Journal of the American College of Cardiology,* vol. 47, pp. 76-84, Jan 3 2006.

[14] S. S. Najjar, "Heart failure with preserved ejection fraction failure to preserve, failure of reserve, and failure on the compliance curve," *Journal of the American College of Cardiology,* vol. 54, pp. 419-21, Jul 28 2009.

[15] W. J. Paulus and J. J. M. van Ballegoij, "Treatment of Heart Failure With Normal Ejection Fraction An Inconvenient Truth!," *Journal of the American College of Cardiology,* vol. 55, pp. 526-537, Feb 9 2010.

[16] S. A. Hunt, "ACC/AHA 2005 guideline update for the diagnosis and management of chronic heart failure in the adult: a report of the American College of Cardiology/American Heart Association Task Force on Practice Guidelines (Writing Committee to Update the 2001 Guidelines for the Evaluation and Management of Heart Failure)," *J Am Coll Cardiol,* vol. 46, pp. e1-82, Sep 20 2005.

[17] T. E. Owan, D. O. Hodge, R. M. Herges, S. J. Jacobsen, V. L. Roger, and M. M. Redfield, "Trends in prevalence and outcome of heart failure with preserved ejection fraction," *The New England journal of medicine,* vol. 355, pp. 251-9, Jul 20 2006.

[18] C. Tribouilloy, D. Rusinaru, H. Mahjoub, V. Souliere, F. Levy, M. Peltier, M. Slama, and Z. Massy, "Prognosis of heart failure with preserved ejection fraction: a 5 year prospective population-based study," *European heart journal,* vol. 29, pp. 339-47, Feb 2008.

[19] T. Bhuiyan and M. S. Maurer, "Heart Failure with Preserved Ejection Fraction: Persistent Diagnosis, Therapeutic Enigma," *Current cardiovascular risk reports,* vol. 5, pp. 440-449, Oct 2011.

[20] M. R. Zile and M. M. Lewinter, "Left ventricular end-diastolic volume is normal in patients with heart failure and a normal ejection fraction: a renewed consensus in diastolic heart failure," *Journal of the American College of Cardiology,* vol. 49, pp. 982-5, Mar 6 2007.

[21] V. Thohan and S. Patel, "The challenges associated with current clinical trials for diastolic heart failure," *Curr Opin Cardiol,* Mar 21 2009.

[22] G. P. Aurigemma, M. R. Zile, and W. H. Gaasch, "Contractile behavior of the left ventricle in diastolic heart failure: with emphasis on regional systolic function," *Circulation,* vol. 113, pp. 296-304, Jan 17 2006.

[23] L. Mandinov, F. R. Eberli, C. Seiler, and O. M. Hess, "Diastolic heart failure," *Cardiovascular research,* vol. 45, pp. 813-25, Mar 2000.

[24] C. Blanche, T. Fumeaux, and R. Polikar, "Heart failure with normal ejection fraction (HFNEF): is it worth considering?," *Swiss medical weekly,* vol. 140, pp. 66-72, Feb 6 2010.

[25] M. R. Zile and D. L. Brutsaert, "New concepts in diastolic dysfunction and diastolic heart failure: Part I: diagnosis, prognosis, and measurements of diastolic function," *Circulation,* vol. 105, pp. 1387-93, Mar 19 2002.

[26] D. Burkhoff, "Pressure-volume loops in clinical research: a contemporary view," *Journal of the American College of Cardiology,* vol. 62, pp. 1173-6, Sep 24 2013.

[27] K. Sagawa, "The end-systolic pressure-volume relation of the ventricle: definition, modifications and clinical use," *Circulation,* vol. 63, pp. 1223-7, Jun 1981.

[28] D. Burkhoff, I. Mirsky, and H. Suga, "Assessment of systolic and diastolic ventricular properties via pressure-volume analysis: a guide for clinical, translational, and basic researchers," *American journal of physiology. Heart and circulatory physiology,* vol. 289, pp. H501-12, Aug 2005.

[29] B. C. Abbott and J. Lowy, "Stress relaxation in muscle," *Proceedings of the Royal Society of London. Series B, Containing papers of a Biological character. Royal Society,* vol. 146, pp. 281-8, Mar 26 1956.

[30] B. C. Abbott and W. F. Mommaerts, "A study of inotropic mechanisms in the papillary muscle preparation," *The Journal of general physiology,* vol. 42, pp. 533-51, Jan 20 1959.

[31] J. G. Pinto and Y. C. Fung, "Mechanical properties of the heart muscle in the passive state," *Journal of biomechanics,* vol. 6, pp. 597-616, Nov 1973.

[32] Y. C. Fung, "Mathematical Representation of Mechanical Properties of Heart Muscle," *Journal of biomechanics,* vol. 3, pp. 381-&, 1970.

[33] T. Varghese, "Quasi-Static Ultrasound Elastography," *Ultrasound clinics,* vol. 4, pp. 323-338, Jul 2009.

[34] S. Gahagnon, Y. Mofid, G. Josse, and F. Ossant, "Skin anisotropy in vivo and initial natural stress effect: a quantitative study using high-frequency static elastography," *Journal of biomechanics,* vol. 45, pp. 2860-5, Nov 15 2012.

[35] S. H. Ibrahim el, "Myocardial tagging by cardiovascular magnetic resonance: evolution of techniques--pulse sequences, analysis algorithms, and applications," *Journal of cardiovascular magnetic resonance : official journal of the Society for Cardiovascular Magnetic Resonance,* vol. 13, p. 36, 2011.

[36] E. A. Zerhouni, D. M. Parish, W. J. Rogers, A. Yang, and E. P. Shapiro, "Human heart: tagging with MR imaging--a method for noninvasive assessment of myocardial motion," *Radiology,* vol. 169, pp. 59-63, Oct 1988.

[37] N. F. Osman, S. Sampath, E. Atalar, and J. L. Prince, "Imaging longitudinal cardiac strain on short-axis images using strain-encoded MRI," *Magnetic resonance in medicine : official journal of the Society of Magnetic Resonance in Medicine / Society of Magnetic Resonance in Medicine,* vol. 46, pp. 324-34, Aug 2001.

[38] A. D. Gilliam and F. H. Epstein, "Automated motion estimation for 2-D cine DENSE MRI," *IEEE transactions on medical imaging,* vol. 31, pp. 1669-81, Sep 2012.

[39] M. C. Petrie, K. Hogg, L. Caruana, and J. J. McMurray, "Poor concordance of commonly used echocardiographic measures of left ventricular diastolic function in patients with suspected heart failure but preserved systolic function: is there a reliable echocardiographic measure of diastolic dysfunction?," *Heart,* vol. 90, pp. 511-7, May 2004.

[40] D. C. Scantlebury and B. A. Borlaug, "Why are women more likely than men to develop heart failure with preserved ejection fraction?," *Current opinion in cardiology,* vol. 26, pp. 562-8, Nov 2011.

[41] c. j. magri, a. cassar, f. stephen, and f. herbert, "Heart Failure with Preserved Ejection Fraction and Diabetes Mellitus," *Journal of Diabetes Research & Clinical Metabolism,* vol. 1, 2012.

[42] M. R. Zile and D. L. Brutsaert, "New concepts in diastolic dysfunction and diastolic heart failure: Part II: causal mechanisms and treatment," *Circulation,* vol. 105, pp. 1503-8, Mar 26 2002.

[43] S. L. Baldwin, M. Yang, K. R. Marutyan, K. D. Wallace, M. R. Holland, and J. G. Miller, "Ultrasonic detection of the anisotropy of protein cross linking in myocardium at diagnostic frequencies," *IEEE transactions on ultrasonics, ferroelectrics, and frequency control,* vol. 54, pp. 1360-9, Jul 2007.

[44] R. Wolk, S. M. Cobbe, M. N. Hicks, and K. A. Kane, "Functional, structural, and dynamic basis of electrical heterogeneity in healthy and diseased cardiac muscle: implications for arrhythmogenesis and anti-arrhythmic drug therapy," *Pharmacology & therapeutics,* vol. 84, pp. 207-31, Nov 1999.

[45] M. O. Biagetti, E. de Forteza, and R. A. Quinteiro, "Differential effects of amiodarone on Vmax and conduction velocity in anisotropic myocardium," *Journal of cardiovascular pharmacology,* vol. 15, pp. 918-26, Jun 1990.

[46] A. Kolipaka, S. R. Aggarwal, K. P. McGee, N. Anavekar, A. Manduca, R. L. Ehman, and P. A. Araoz, "Magnetic resonance elastography as a method to estimate myocardial contractility," *Journal of magnetic resonance imaging : JMRI,* vol. 36, pp. 120-7, Jul 2012.

[47] A. Kolipaka, P. Araoz, K. P. McGee, A. Manduca, and R. L. Ehman, "In Vivo Cardiac MR Elastography in a Single Breath Hold," *Proceedings of the 18th Annual Meeting of ISMRM, Stockholm, Sweden,* p. 519, 2010.

[48] A. Kolipaka, P. A. Araoz, K. P. McGee, A. Manduca, and R. L. Ehman, "Magnetic resonance elastography as a method for the assessment of effective myocardial stiffness throughout the cardiac cycle," *Magnetic resonance in medicine : official journal of the Society of Magnetic Resonance in Medicine / Society of Magnetic Resonance in Medicine,* vol. 64, pp. 862-70, Sep 2010.

[49] A. Kolipaka, K. P. McGee, S. R. Aggarwal, Q. Chen, N. Anavekar, A. Manduca, R. L. Ehman, and P. Araoz, "A Feasibility Study: MR Elastography as a Method to Compare Stiffness Estimates in Hypertrophic Obstructive Cardiomyopathy and in Normal Volunteers," *Proceedings of the 19th Annual Meeting of ISMRM, Montreal, Canada,* 2011.

[50] A. Kolipaka, K. P. McGee, S. R. Aggarwal, Q. Chen, N. Anavekar, A. Manduca, R. L. Ehman, and P. Araoz, "Regional quantification of Myocardial Stiffness using MR Elastography," *Proceedings of the 19th Annual Meeting of ISMRM, Montreal, Canada,* p. 15, 2011.

[51] A. Kolipaka, K. P. McGee, P. A. Araoz, K. J. Glaser, A. Manduca, and R. L. Ehman, "Evaluation of a rapid, multiphase MRE sequence in a heart-simulating phantom," *Magnetic resonance in medicine : official journal of the Society of Magnetic Resonance in Medicine / Society of Magnetic Resonance in Medicine,* vol. 62, pp. 691-8, Sep 2009.

[52] A. Kolipaka, K. P. McGee, P. A. Araoz, K. J. Glaser, A. Manduca, A. J. Romano, and R. L. Ehman, "MR elastography as a method for the assessment of myocardial stiffness: comparison with an established pressure-volume model in a left ventricular model of the heart," *Magnetic resonance in medicine : official journal of the Society of Magnetic Resonance in Medicine / Society of Magnetic Resonance in Medicine,* vol. 62, pp. 135-40, Jul 2009.

[53] A. Kolipaka, K. P. McGee, A. Manduca, N. Anavekar, R. L. Ehman, and P. A. Araoz, "In vivo assessment of MR elastography-derived effective end-diastolic myocardial stiffness under different loading conditions," *Journal of magnetic resonance imaging : JMRI,* vol. 33, pp. 1224-8, May 2011.

[54] A. Kolipaka, K. P. McGee, A. Manduca, A. J. Romano, K. J. Glaser, P. A. Araoz, and R. L. Ehman, "Magnetic resonance elastography: Inversions in bounded media," *Magnetic resonance in medicine : official journal of the Society of Magnetic Resonance in Medicine / Society of Magnetic Resonance in Medicine,* vol. 62, pp. 1533-42, Dec 2009.

[55] K. J. Glaser, A. Manduca, and R. L. Ehman, "Review of MR elastography applications and recent developments," *Journal of magnetic resonance imaging : JMRI,* vol. 36, pp. 757-74, Oct 2012.

[56] A. Manduca, T. E. Oliphant, M. A. Dresner, J. L. Mahowald, S. A. Kruse, E. Amromin, J. P. Felmlee, J. F. Greenleaf, and R. L. Ehman, "Magnetic resonance elastography: non-invasive mapping of tissue elasticity," *Medical image analysis,* vol. 5, pp. 237-54, Dec 2001.

[57] A. Romano, R. Mazumder, S. Choi, B. D. Clymer, R. D. White, and A. Kolipaka, "Waveguide Magnetic Resonance Elastography of the Heart," *Proceedings of the 21st Annual Meeting of ISMRM, Utah, USA,* p. 2431, 2013.

[58] A. J. Romano, P. B. Abraham, P. J. Rossman, J. A. Bucaro, and R. L. Ehman, "Determination and analysis of guided wave propagation using magnetic resonance elastography," *Magn Reson Med,* vol. 54, pp. 893-900, Oct 2005.

[59] A. Romano, P. B. Abraham, S. I. Ringleb, P. J. Rossman, J. A. Bucaro, and R. L. Ehman, "Determination of Anisotropic Velocity Profiles in Muscle Using Wave-Guide Constrained

Magnetic Resonance Elastography," *Proceedings of the 14th Annual Meeting of ISMRM, Seattle, Washington, USA,* p. 1725, 2006.

[60] A. Romano, M. Scheel, S. Hirsch, J. Braun, and I. Sack, "In vivo waveguide elastography of white matter tracts in the human brain," *Magn Reson Med,* vol. 68, pp. 1410-22, Nov 2012.

[61] A. Romano, J. Guo, T. Prokscha, T. Meyer, S. Hirsch, J. Braun, I. Sack, and M. Scheel, "In vivo waveguide elastography: Effects of neurodegeneration in patients with amyotrophic lateral sclerosis," *Magnetic resonance in medicine : official journal of the Society of Magnetic Resonance in Medicine / Society of Magnetic Resonance in Medicine,* Dec 17 2013.